

Low temperature superplasticity of the ECAP Al7075-based alloy

P. Málek^{1,2}, O. Molnárová^{1,2,†}, P. Lejček¹

[†]molnarova@fzu.cz

¹Institute of Physics, Academy of Sciences of the Czech Republic, Na Slovance 2, 18221 Prague 8, Czech Republic

²Charles University, Department of Physics of Materials, Ke Karlovu 5, 12116 Prague 2, Czech Republic

Using equal channel angular pressing (ECAP) at 120 °C, a sub-microcrystalline structure was prepared in the Al7075 alloy modified by the addition of 0.2 wt. % Sc and 0.11 wt. % Zr. This relatively low ECAP temperature resulted in a very fine grain size of 0.5 µm, however, this microstructure was not stable and a grain growth started already at 300 °C. Consequently, the superplastic behaviour was not observed at temperatures above 400 °C which are typical for the Al7075-type alloys. The tensile tests performed at temperatures below 300 °C revealed enhanced ductility — elongation exceeding 300% was observed in this material already at 200 °C. In order to verify whether such behaviour can be considered as so called “low temperature superplasticity”, a microstructure investigation was performed using scanning electron microscopy, electron back scatter diffraction, transmission electron microscopy, and atom force microscopy. These experiments revealed that the deformation mechanism was similar to that observed in “true” superplasticity. Grain boundary sliding played still an active role. The elongation of individual grains during straining was significantly lower in comparison with the overall sample elongation, nevertheless it documented the contribution of dislocation slip to the deformation mechanism.

Keywords: Al7075 alloy, ECAP, low temperature superplasticity, microstructure investigation.

1. Introduction

The phenomenon of superplasticity is known since 1934 [1], however, a proper investigation of the deformation mechanism responsible for superplastic behaviour started in 70th [2,3]. The book of Prof. Kaibyshev brings the description of basic deformation processes which might be expected during superplastic deformation and especially shows their interconnection. The pioneering publications proposed the ductility of 200% and the value of strain rate sensitivity parameter $m=0.3$ to be the bottom limits of superplastic behaviour. Simultaneously the necessary prerequisites for superplastic behaviour were postulated — a fine-grained structure (grain size in the micrometer range), an elevated straining temperature (above approximately $0.5 T_m$), and a suitable strain rate (typically $10^{-4} - 10^{-3} \text{ s}^{-1}$).

The development of new technologies for processing of sub-micrometer grained materials (e.g. methods of severe plastic deformation [4]) revealed that the superplastic region could be displaced to significantly higher strain rates (10^{-2} to 10^{-1} s^{-1}) (e.g. [5]). Numerous researchers confirmed that the deformation mechanism of the so called high-strain-rate superplasticity was the same as that observed previously in the micrometer grained materials. Less attention was paid to the position of the superplastic region on the temperature scale. Whereas e.g. dilute Zn-Al alloys exhibit superplasticity already at temperatures below $0.5 T_m$ [6], most Al-based alloys are superplastic at much higher temperatures, typically between $0.7 T_m$ and $0.8 T_m$, i.e. above approximately 400 °C (e.g. [7]). However, a reduction in the grain size can be expected to result also in a displacement of the superplastic region to lower temperatures.

Low temperature superplasticity was reported in many Al-based alloys. Most of them are alloys rich in Mg. McNelley et al. reported ductility of 400% in an Al-Mg-Mn alloy [8], Turba et al. observed ductility of 410% in an Al-Mg-Sc-Zr alloy [9], both at 300 °C. Hsiao et al. found the same ductility even at 250 °C in the Al5083 alloy [10] and Ota et al. reported ductility over 400% even at 200 °C in the Al-Mg-Sc prepared using equal channel angular pressing (ECAP) [11] and considered this value as the highest one in the low temperature superplasticity regime. The maximum values of the parameter m were generally between 0.3 and 0.4. In all these cases the initial microstructure was extremely fine grained with the grain size usually below 1 µm. In the Al-Zn-Mg-Cu based alloys, the low temperature superplasticity was observed in materials prepared using friction-stir-processing [12,13]. The grain size of these materials was less than 1 µm and the maximum values of ductility in the low-temperature region were 266% at 220 °C in [12] and 350% at 200 °C in [13]. The parameter m was slightly above 0.3 in both cases.

A sub-micrometer grain size can also be produced in the Al7075 alloy using ECAP [14]. It was shown in [15] that a reduction in the ECAP temperature down to 120 °C resulted in a grain size of 0.5 µm. However, this very fine-grained structure was not stable at elevated temperatures and a grain growth started already at 300 °C. Consequently, the true superplastic behaviour could not be observed at typical temperatures above 400 °C. On the other side, the ductility reached the values close to 200% already at temperatures 200 °C and 300 °C [16] which suggested the phenomenon of low temperature superplasticity. In order to confirm this suggestion, the Al7075 alloy modified by the additions of Sc and Zr was prepared using ECAP and

strained at temperatures below 300 °C. An investigation of the deformation structure of samples strained in the range of low temperature superplasticity was performed in order to elucidate the deformation mechanism at these conditions.

2. Materials and methods

The commercial Al7075 alloy with a chemical composition (in wt. %) of 5.88 Zn, 2.45 Mg, 1.32 Cu, 0.37 Fe, 0.35 Si, 0.19 Cr, and 0.17 Mn was modified by additions of 0.20 Sc and 0.11 Zr to form the $Al_3(Sc,Zr)$ particles contributing to the microstructure stabilization. The material in a soft state (i.e. after annealing at 400 °C for 8 hours) was processed by ECAP at 120 °C. The rectangular samples (10 × 10 mm) were pressed in 6 passes through a die consisting of two channels intersecting at 90° with a B_c rotation between individual passes. For comparison, the same material was processed by ECAP at 170 °C.

The rectangular tensile samples with a gauge length of 17 mm and a cross section of 6 × 1 mm² were machined from ECAP billets parallel to the pressing direction. Tensile tests were carried out using an Instron 5882 machine at a constant crosshead speed at several relatively low temperatures. The method of strain rate changes was used to determine the parameter m values.

The evolution of the grain structure during straining was studied using the electron back scatter diffraction (EBSD) method. The samples were strained to a certain strain, then mechanically polished, and finally ion polished using a LEICA EM RES102 ion polisher. The scanning electron microscope (SEM) FEI Quanta 200 F equipped with a field emission cathode was used. The orientation image maps from EBSD investigation were processed using OIM Analysis program. The step size of EBSD measurement was 0.08 µm.

In order to follow the changes in the deformation structure caused by straining, the tensile samples were mechanically polished and then strained to different strains. The surface of strained samples was investigated both by the SEM and by the atom force microscopy (AFM) method using a Bruker Dimension Edge device. Finer microstructural details were investigated using transmission electron microscopy (TEM). The foils were prepared by electrochemical thinning using a double-jet polisher in a solution of 33% nitric acid in methyl alcohol at 15 V and –15 °C. The FEI Tecnai TF20 X-twin microscope was used.

3. Experimental results

The true stress vs. elongation curves obtained for temperatures between 150 °C and 250 °C are shown in Fig. 1a. An extremely high ductility reaching 340% was observed at 200 °C, simultaneously with the value of the parameter $m = 0.3$. Lower values of ductility and of parameter m were observed at temperatures 150 °C and 250 °C. The shape of the stress-strain curves is similar to that observed for true superplastic behaviour observed at much higher straining temperature in the sample processed by ECAP at 170 °C (Fig. 1b). A slight softening during straining is probably caused by a non-homogeneous strain distribution resulting in a diffuse necking.

The grain structures of samples strained to 50% of elongation in the range of “low temperature” and “true” superplasticity are compared in Fig. 2. A smaller grain size and a more homogeneous distribution of grain sizes were observed in the sample strained at 200 °C.

Fig. 3 shows the EBSD images for samples strained to different strains at 200 °C, i.e. in the range of the low temperature superplasticity. The vertical direction in these figures is parallel to the tensile axis. The mean grain size and the grain aspect ratio values are summarized in Table 1. Only a very small increase in the grain size occurs during straining. The maximum elongation of individual grains along the tensile axis observed in the sample strained to fracture (340%) does not exceed 50%.

Table 1: The influence of straining on the grain size and grain aspect ratio for the samples after ECAP at 120 °C strained at 200 °C and strain rate of 2.10^{-4} s^{-1} .

Elongation, %	Grain size, µm	Grain aspect ratio
20	0.63 ± 0.17	1.0
50	0.75 ± 0.24	1.2
100	0.98 ± 0.38	1.5
340	0.93 ± 0.30	1.5

Whereas dislocation slip is the main deformation mechanism in the plastic deformation of Al alloys at room temperature, grain boundary sliding brings the largest contribution to the overall strain during superplastic deformation [2,3]. In order to elucidate the deformation mechanism in the range of low temperature superplasticity,

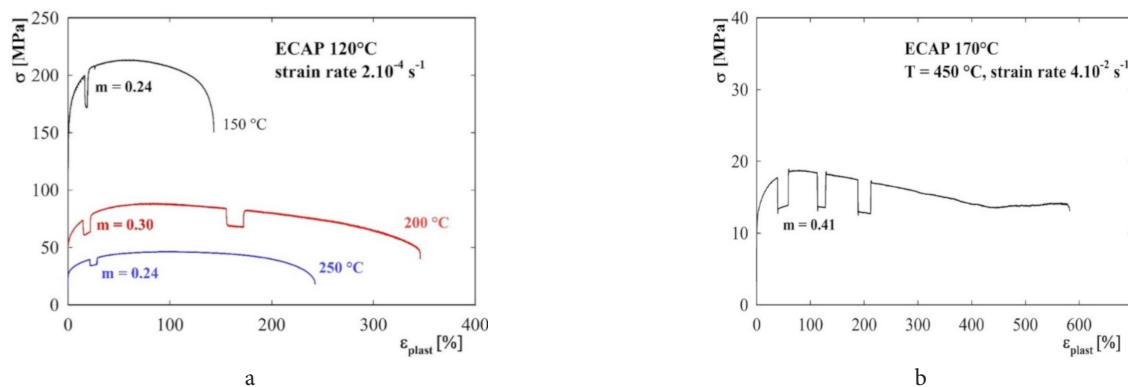


Fig. 1. Stress-strain curves for different temperatures, samples after ECAP at 120 °C (a), and at 170 °C (b).

the surface of previously polished tensile samples strained to 50 or 100% of elongation was studied using SEM and AFM methods. Fig. 4 documents clearly mutual displacements of neighbouring grains, i.e. the operation of grain boundary sliding in secondary electron imaging (SE). The comparison of both samples shows that the number of grain boundaries involved in grain boundary sliding increases with increasing strain, so that sliding is more homogeneously distributed.

Atom force microscopy yields quantitative information on the extent of individual grain displacements. Figs. 5a,b show the surfaces of both strained samples in the mode where different shades are attributed to different gradients in the z -coordinate. The individual grains are visualised through displacements and rotations of grains. In the sample strained to 50%, the sliding is concentrated along some interconnected grain boundaries. An increase in the strain results in a homogenization of the sliding within the sample.

Fig. 6 shows the topographic line profiles and confirms the finding mentioned above — more grain boundaries

are involved in grain boundary sliding with increasing strain. Simultaneously the surface roughness increases, i.e. individual displacements increase up to $0.2\ \mu\text{m}$.

The elongation of individual grains during straining observed by EBSD method suggests that the slip of lattice dislocation is also engaged in the deformation process. TEM investigation was performed to judge the role of lattice dislocations. It was found that majority of grains did not contain lattice dislocations. Fig. 7 shows the micrographs of the sample strained at $200\ ^\circ\text{C}$ to 100% (a) and the grip region of the same sample which was not strained (b). In Fig. 7, such grains were selected where lattice dislocations are pinned by second phase particles. Fig. 7a reveals the interactions of lattice dislocations with grain boundaries and also pile-ups of dislocations at the boundary. Grains with a similar dislocation density can be found also in the grip region (Fig. 7b). The comparison of both samples documents a negligible effect of straining on the dislocation structure.

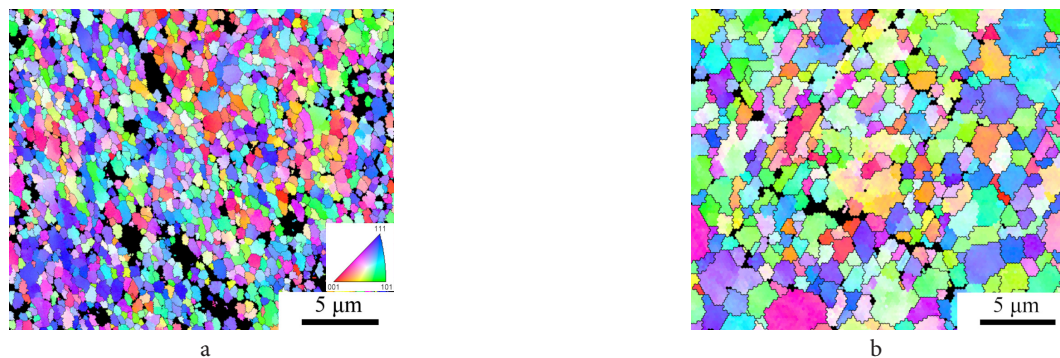


Fig. 2. The EBSD micrographs of ECAPed samples. The sample after ECAP at $120\ ^\circ\text{C}$ strained to 50% at $200\ ^\circ\text{C}$ at the strain rate of $2 \cdot 10^{-4}\ \text{s}^{-1}$ (a); the sample after ECAP at $170\ ^\circ\text{C}$ strained to 50% at $450\ ^\circ\text{C}$ at the strain rate of $4 \cdot 10^{-2}\ \text{s}^{-1}$.

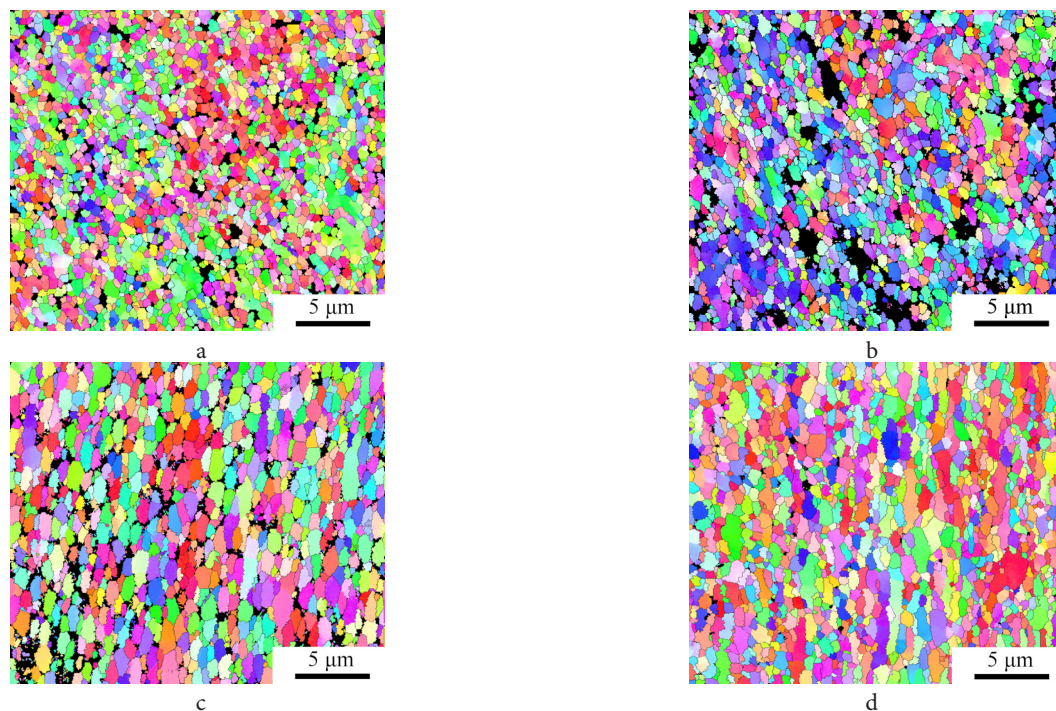


Fig. 3. The EBSD micrographs of the samples after ECAP at $120\ ^\circ\text{C}$, strained at $200\ ^\circ\text{C}$ and strain rate of $2 \cdot 10^{-4}\ \text{s}^{-1}$ to: 20% (a), 50% (b), 100% (c), 340% (d).

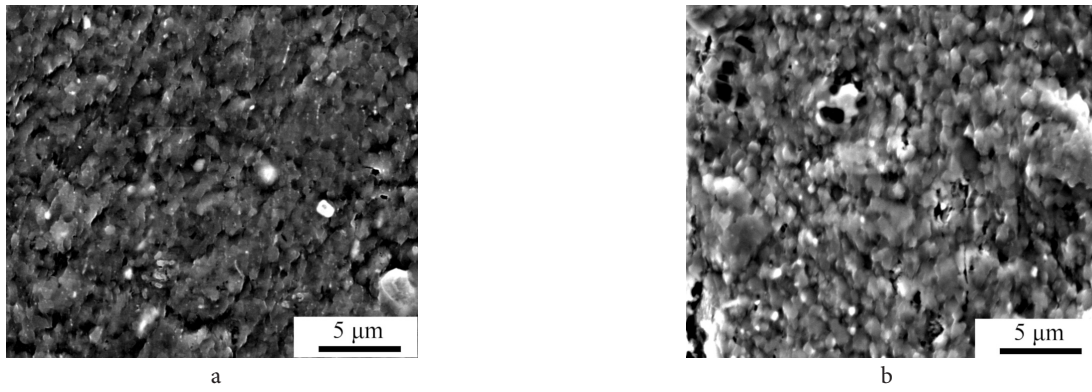


Fig. 4. The SEM micrographs of the samples after ECAP at 120 °C, strained at 200 °C and strain rate of 2.10^{-4} s^{-1} to: 50% (a), 100% (b), SE.

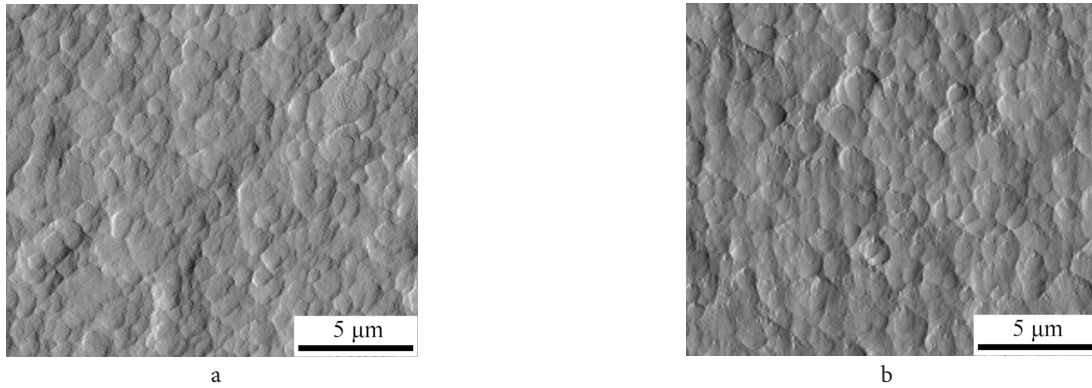


Fig. 5. The AFM micrographs of the samples after ECAP at 120 °C, strained at 200 °C and strain rate of 2.10^{-4} s^{-1} to: 50% (a), 100% (b).

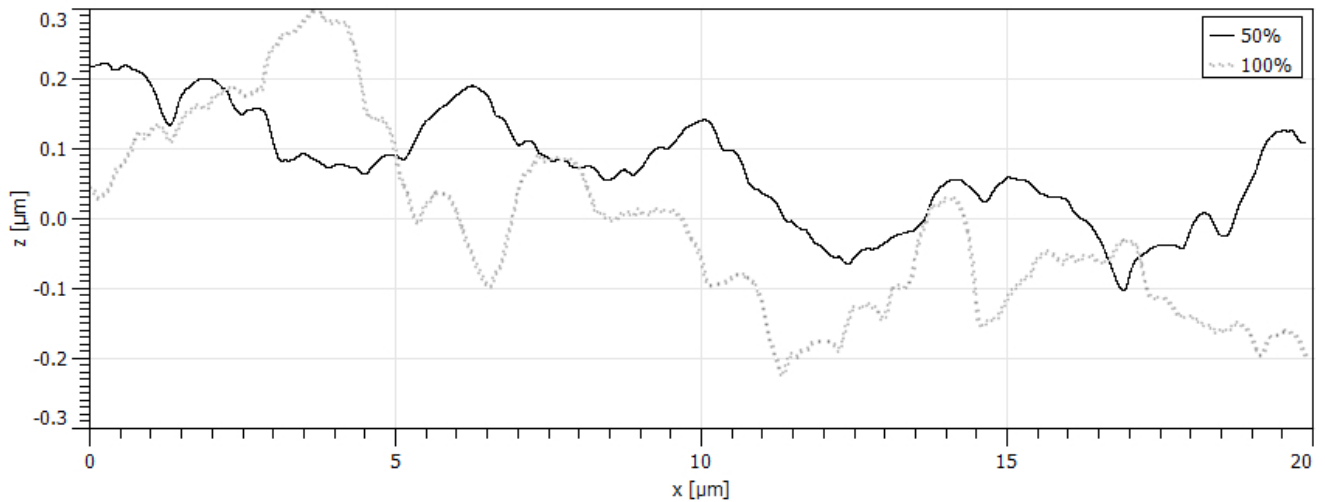


Fig. 6. The topographic line profiles of the samples after ECAP at 120 °C, strained at 200 °C and strain rate of 2.10^{-4} s^{-1} to 50 and 100%.

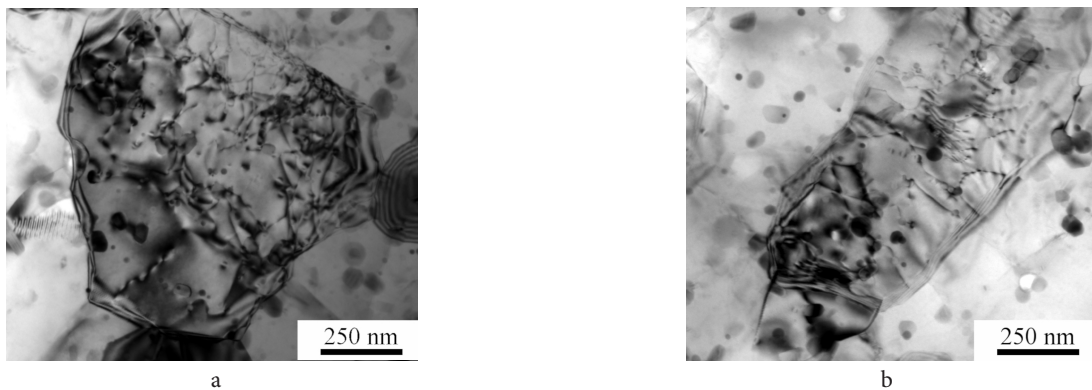


Fig. 7. The TEM micrographs of the sample after ECAP at 120 °C, strained at 200 °C and strain rate of 2.10^{-4} s^{-1} to 100% (a), the corresponding grip region (b).

4. Discussion

There is a general question whether the deformation characteristics demonstrated in Fig. 1 can be considered as superplastic. As mentioned in the Introduction, the ductility of 200% and the value of the parameter $m=0.3$ were previously considered as bottom limits of superplastic behaviour [2,3]. New criteria (ductility over 400% and parameter $m=0.5$) were postulated as bottom limits of superplasticity in [17]. This change was based especially on the requirement to exclude some coarse grained Al-Mg alloys with enhanced ductility from the group of superplastic materials. However, these criteria seem to be too strong and especially the value of the parameter $m=0.5$ cannot be reached in many “true” superplastic materials (e.g. [15]). All experimental results obtained in the range of low-temperature superplasticity do not also meet these criteria. Therefore, these new criteria have to be used with great care and additional characteristics have to be considered in order to distinguish between superplastic deformation and other types of deformation resulting in an enhanced ductility. Especially the microstructural characteristics typical for different deformation mechanisms have to be verified.

It is generally accepted that grain boundary sliding is the main deformation mechanism during superplastic deformation [2,3]. This deformation mechanism was clearly observed in our alloy. It seems that sliding occurs in a cooperative manner where groups of several grains slide as units. The extent of sliding and the number of grain boundaries involved in this process increases during straining. On the other side, the contribution of dislocation slip is considered to be relatively limited during superplastic deformation [2,3]. An absence of grain elongation after superplastic straining and very small dislocation densities inside the grains are the main arguments for this statement. In our material, the grains revealed some elongation along the tensile direction, however, the deformation of individual grains was several times lower as compared to the overall sample elongation. A low dislocation density was typical for a majority of grains. Some dislocations were observed only at places where they were pinned by second phase particles. Interactions of lattice dislocations with grain boundaries were also observed which suggested that these dislocations could be probably easily absorbed by grain boundaries. It can be concluded that the contribution of dislocation slip in the low temperature superplasticity is higher than in the true “high temperature” superplasticity. However, grain boundary sliding remains the main deformation mechanism in our material strained at relatively low temperatures and therefore, its deformation can be considered as superplastic. The extremely fine grain size connected with increased number of grain boundaries seems to be responsible for this extension of superplastic range to lower straining temperatures.

5. Conclusions

- The Al7075 alloy modified by the additions of Sc and Zr processed by 6 passes of ECAP at 120 °C exhibits „low temperature” superplasticity with the maximum elongation of 340% and parameter $m=0.3$ at the straining temperature of 200 °C.

- The original grain size of 0.5 µm is relatively stable and remains below 1 µm after straining at this temperature. The maximum grain elongation of 50% was observed in the sample strained to the overall strain of 340%.

- The deformation relief becomes rougher with increasing strain. The typical displacements of neighbouring grains due to grain boundary sliding are between 0.1 and 0.2 µm in the sample strained to 100%. The grains slide in groups at lower strain. A tendency to sliding of individual grains was observed with increasing strain.

- The density of dislocations is very low even after 100% of elongation, individual dislocations were observed only at coarser second phase particles.

- The deformation mechanism of the “low temperature” superplasticity is similar to that observed in true superplastic materials. Grain boundary sliding plays still an active role, however, its contribution to the overall strain is probably lower. On the other side, a partial elongation of individual grains during straining documents that the contribution of lattice dislocations slip cannot be neglected.

Acknowledgements. This research was supported by the Czech Science Foundation under grant P108/12/G043 and by the project LM2015087 of the Czech Ministry of Education, Youth, and Sports. One of authors (M. P.) expresses thanks to Prof. O. A. Kaibyshev for encouraging at the start of his research in the field of structural superplasticity.

References

1. C.E. Pearson. J. Inst. Metals. 54, 111 (1934).
2. O.A. Kaibyshev. Plastichnost' i sverchplastichnost' metallov. Moscow, Metallurgia (1975) 280 p. (in Russian)
3. J.W. Edington, K.N. Melton, C.P. Cutler. Prog. Mater. Sci. 21, 61 (1976).
4. R.Y. Valiev, R.K. Islamgaliev, I.V. Alexandrov. Prog. Mater. Sci. 45, 103 (2000).
5. Z. Horita, M. Furukawa, M. Nemoto, A.J. Barnes, T.G. Langdon. Acta mater. 48, 3633 (2000).
6. P. Málek, P. Lukáč. Czech. J. Phys B. 36, 498 (1986).
7. O.A. Kaibyshev. Sverkhplastichnost' Promyshlennykh Splavov (Superplasticity of Commercial Alloys). Moscow, Metallurgia (1984) 264 p. (in Russian)
8. T.R. McNelley, E.-W. Lee, M.E. Mills. Met. Trans. 17A, 1035 (1986).
9. K. Turba, P. Málek, M. Cieslar. Mater. Sci. Eng. A. 462, 91 (2007).
10. I.C. Hsiao, J.C. Huang. Scripta Mater. 40, 697 (1999).
11. S. Ota, H. Akamatsu, K. Neishi, M. Furukawa, Z. Horita, T.G. Langdon. Met. Trans. 43, 2364 (2002).
12. I. Charit, R.S. Mishra. Acta Mater. 53, 4211 (2005).
13. F.C. Liu, Z.Y. Ma. Scripta mater. 58, 667 (2008).
14. R.Y. Valiev, M.J. Zehetbauer, Z. Estrin, H.W. Hoepfel, Z. Ivanisenko, H. Hahn, G. Wilde, H.J. Roven, X. Sauvage, T.G. Langdon. Adv. Eng. Mater. 9, 527 (2007).
15. P. Málek, K. Turba, M. Cieslar, P. Hrcuba. IJMR. 104, 3 (2013).
16. P. Lukáč, K. Turba, P. Málek, M. Cieslar. IJMR. 100, 847 (2009).
17. T.G. Langdon. J. Mater. Sci. 44, 5998 (2009).